Effect of edge reconstruction and passivation on zero-energy states and magnetism in triangular graphene quantum dots with zigzag edges

O. Voznyy,[1] A. D. Güçlü,[1] P. Potasz,[1,2] and P. Hawrylak[1]
[1]*Institute for Microstructural Sciences, National Research Council of Canada, Ottawa, Canada*
[2]*Institute of Physics, Wroclaw University of Technology, Wroclaw, Poland*
(Received 13 October 2010; revised manuscript received 2 March 2011; published 14 April 2011)

We present the results of *ab initio* calculations of the effect of reconstruction and passivation of zigzag edges on the electronic and magnetic properties of triangular graphene quantum dots. We find that, similarly to nanoribbons, hydrogen-passivated ideal zigzag edges are energetically favored over the pentagon-heptagon zigzag. However, the reconstructed edge is more stable in the absence of hydrogen, thus, delayed passivation with H may lock the dot in such an unfavorable configuration. Both hydrogen-passivated edge morphologies lead to a band of states at the Fermi level. Unlike in nanoribbons, this quasidegenerate band results in net spin polarization for structures with zigzag edge of all sizes studied here. For triangular dots with pentagon-heptagon zigzag edge, a larger width of the zero-energy band is predicted, leading to the loss of net magnetization.

DOI: 10.1103/PhysRevB.83.165417 PACS number(s): 73.22.Pr, 68.65.Pq, 75.75.−c

Graphene, an atomically thick honeycomb lattice of carbon atoms, exhibits fascinating properties due to the relativistic-like nature of quasiparticle dispersion close to the Fermi level.[1–5] Graphene's potential for nanoelectronics applications, particularly magnetization of edges, and its use for spintronics motivated considerable amount of research in graphene nanoribbons[6–10] and, more recently, graphene quantum dots.[11–25] Large optical absorptivity, tunable electronic levels, high charge mobility, and nontoxicity make graphene nanostructures attractive also for photovoltaic applications.[26]

In low-dimensional graphene structures, the overall shape and the character of the edges drastically affect the electronic properties near the Fermi level.[25,27–29] In particular, theoretical models predict that, in triangular graphene quantum dots (TGQDs) with exclusively zigzag edges, the energy spectrum near the Fermi level collapses to a band of degenerate states, isolated from the rest of the spectrum by a well-defined gap, with states predominantly localized on the edges.[16–21,23–25] It was shown that, unlike in graphene nanoribbons that have no net magnetic moment, in this band of degenerate states, strong electron-electron interactions lead to ferromagnetism and peculiar magnetic[19,21,24,30] and optical[22,25] properties, e.g., magnetic moment proportional to the dot size and controlled by an external gate. TGQDs might also offer additional advantages for third-generation solar cells utilizing the presence of the intermediate band in the gap[31] and multi-exciton generation (MEG).[32] MEG was already demonstrated in carbon nanotubes,[33,34] while a recent theoretical study[35] suggests that it is also possible in graphene QDs, and that localization of states on the edges increases MEG efficiency.

Despite the fact that TGQDs with zigzag edges have not been demonstrated yet, recent experimental works suggest that they are conceivable in the future. Typically, the solution-derived organic chemistry methods produce graphene nanostructures with H-passivated edges with a predominantly armchair structure.[10,36,37] Other techniques, such as etching lithography or mechanical exfoliation, result in nanostructures with a mixture of zigzag and armchair edges, and their reconstructed counterparts. The edges' morphology is found to be highly dynamic under nonequilibrium preparation conditions, and interconversion between different types of edge reconstructions is often observed.[29,38–42] Techniques for preparation of graphene nanostructures with controlled-edge morphology are constantly emerging, e.g., nanotube unzipping[43] and Joule heating,[40,44] and some of them, such as anisotropic etching using Ni (Ref. 46) or Co (Ref. 47) nanoparticles and carbothermal decomposition of SiO_2,[45] can already produce exclusively zigzag edges and triangular shapes. Other alternatives based on patterned hydrogenation rather than etching were also proposed.[48]

Theoretical predictions for infinite edges suggest that, with hydrogen passivation, armchair configuration is the most favorable one, with only a slight energy advantage over zigzag (ZZ). Without H, a reconstructed edge terminated by pentagon-heptagon pairs (ZZ_{57}) is predicted to be the lowest in energy, followed by armchair.[8,39,49,50] For finite-size structures, however, confinement effects and the presence of corners would affect the stability of the overall structure and the preferred edge morphology. For example, ZZ edges are suggested to be dominating for small carbon clusters, both with and without H passivation, while injection of pentagon and heptagon defects may lower the total energy for some structures.[51]

Determining the degree of edge passivation (one, two, or no H atoms attached to edge carbon[8]) in experimental structures is still complicated.[42,45] Under the damaging high flux of electrons in transmission electron microscopy (TEM) there is, likely, no H. A consequent hydrogenation of such unpassivated edges is possible.[8,27] Interconversion between reconstructions requires overcoming high-energy barriers, even for nonpassivated carbon edges.[44] Thus, locking in a nonoptimal configuration remains quite possible. So far, only TGQDs with ideal H-passivated ZZ and armchair edges were studied. Effects of pentagons and heptagons injection, leading to mixing of the sublattices, has not been addressed yet.

In this paper, using *ab initio* methods, we investigate the robustness of TGQD properties of interest (zero-energy states and magnetism) versus edge reconstructions and passivation as a function of size. We use the most feasible with current manufacturing technique reconstructions (ZZ and ZZ_{57}),[38,39,41]

while our conclusions are expected to be general for any configuration of pentagon-heptagon defects. We discover the loss of magnetization in ZZ_{57} due to the increased width of the zero-energy band. A more detailed study reveals why, in larger ZZ TGQDs, with similar band dispersion, magnetization is not affected.

Calculations have been performed within the density functional theory approach as implemented in the SIESTA code.[52] We have used the generalized gradient approximation (GGA) with the Perdew-Burke-Ernzerhof (PBE) exchange-correlation functional,[53] double-ζ plus polarization (DZP) orbital bases for all atoms (i.e., $2s$, $2p$, and $2d$ orbitals for carbon, thus, both σ and π bonds are included on equal footing), Troullier-Martins norm-conserving pseudopotentials to represent the cores, 300-Ry real-space mesh cutoff for charge density (with symmetrization sampling to further improve the convergence), and a supercell with at least 20 Å of vacuum between the periodic images of the TGQDs. Geometries were optimized until the forces on atoms below 40 meV/Å were reached, and exactly the same geometries were used for the comparison of total energies of the ferromagnetic (FM) and antiferromagnetic (AFM) configurations. Our optimized C-C bond length for bulk graphene of 1.424 Å overestimates the experimental value by ~3%, typical for GGA.

Figure 1 shows the different TGQD structures considered in this paper. Depending on the parity of the amount of atoms in the edge of TGQD, the requirement of the ZZ_{57} reconstruction of the edge leads to several possible structures. The three rings at the corner can have 5-7-5, 7-6-5, or 6-6-5 arrangements, presented in Figs. 1(b)–1(d) (for the sake of comparison of total energies, we investigate only those reconstructions conserving the amount of atoms). Among reconstructed corners, only the structure in Fig. 1(b) conserves the mirror symmetry of the TGQD; however, according to our calculations, it is the least stable due to strong distortion of the corner cells. Thus, in the remainder of this paper, we will be presenting results utilizing the configuration shown in Fig. 1(c) for an even, and that in Fig. 1(d) for an odd, number of atoms n on a side of the triangle.

Passivation by hydrogen is an important requirement for the observation of the band of nonbonding states. Our calculations show that, without hydrogen passivation, the π bonds hybridize with the σ bonds on the edge, destroying the condition of the well-defined equivalent bonds on a bipartite lattice and thus the zero-energy band itself. In Fig. 2(a), we address the stability of hydrogen passivation for ZZ and ZZ_{57} edges on the example of a triangle with $n = 8$ atoms on a side (97 carbon atoms total and number of passivating hydrogens $N_H = 3n + 3 = 27$). For hydrogen-passivated structures, ZZH is 0.3 eV per hydrogen atom more stable than $ZZ_{57}H$ since, in the latter structure, the angles between the σ bonds significantly deviate from the ideal 120° and the total energy is affected by strain. In the absence of hydrogen, however, the structure has to passivate the dangling σ bonds by itself, e.g., by reconstructing the edge. Indeed, the ZZ_{57} reconstruction becomes 0.4 eV more stable. It is important to note that hydrogen passivation is a favorable process for both structures, even relative to the formation of H_2 molecules, and not only atomic hydrogen (i.e., formation of the H-H bond can not compensate the energy loss due to breaking the C-H bond) [Fig. 2(a)]. The same conclusions hold for larger TGQDs as well. Thus, the H-passivated edge, required for magnetism, is easily achievable and we will present further only the results for hydrogen-passivated structures omitting the index H (i.e., use ZZ instead of ZZH). These results are also consistent with the ones for infinite edges in graphene nanoribbons.[8,49,50] In Fig. 2(b), we investigate the relative stability of hydrogen-passivated ZZ and ZZ_{57} structures as a function of the linear size of the triangles. The largest TGQD that we have studied has $n = 23$ atoms on a side of the triangle (622 carbon atoms total). The fact that the energy per edge atom increases with size signifies that the bulk limit has not yet been reached. Clearly, the ZZ structure remains the ground state for the range of sizes studied here. Nevertheless, since most of the current experimental techniques involve the unpassivated edge, for which ZZ_{57} is more stable, its consequent hydrogenation may propagate the reconstruction into the final structure, where it may be locked due to high interconversion barrier.[44]

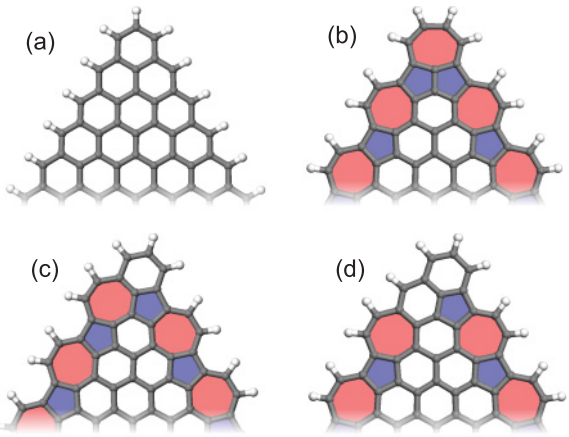

FIG. 1. (Color online) Triangular graphene quantum-dot edge configurations considered in this paper: (a) Ideal zigzag edges ZZ, (b) ZZ_{57} reconstruction with pentagon-heptagon-pentagon corner configuration, (c) ZZ_{57} reconstruction with heptagon-hexagon-pentagon corner, and (d) ZZ_{57} reconstruction with hexagon-hexagon-pentagon corner.

It was shown previously that the number of states in the zero-energy band equals the difference between the number

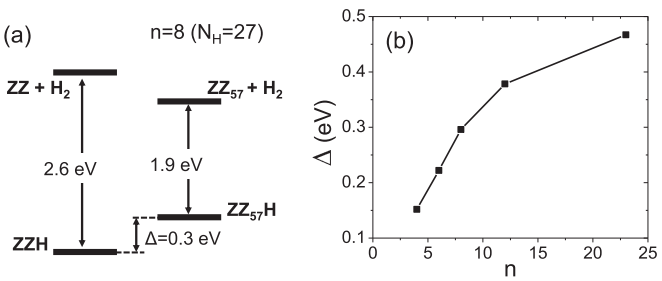

FIG. 2. (a) Relative total energies of hydrogen-passivated and nonpassivated TGQDs with reconstructed and nonreconstructed edges for the case of $n = 8$ ($N_H = 27$). (b) Total energy difference between hydrogen-passivated ZZ_{57} and ZZ configurations as a function of the number of atoms on a side of the triangle. Presented values are energy per hydrogen atom.

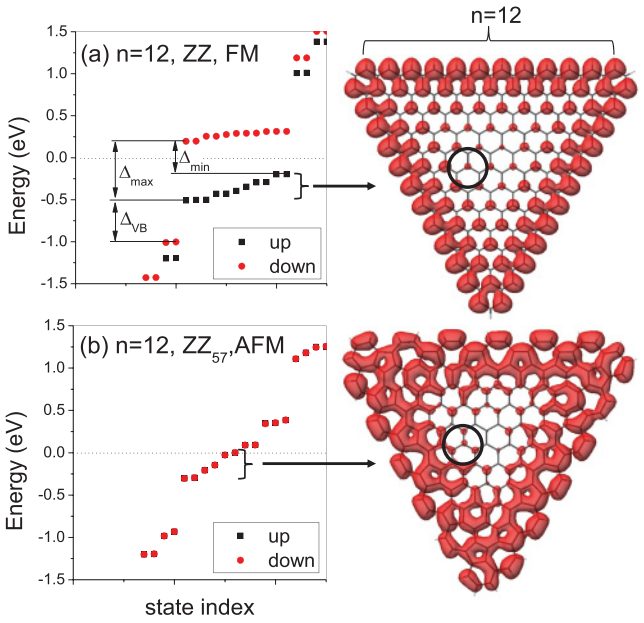

FIG. 3. (Color online) Energy spectra of the ground states for (a) ZZ and (b) ZZ_{57} configurations for a hydrogen-passivated triangular dot with $n = 12$. Spin-up states are shown in black squares and spin-down states are shown in red circles. On the right-hand side, charge densities of the filled part of zero-energy bands are shown. Circular outlines show the population of only one sublattice in the ZZ structure and both sublattices in ZZ_{57}.

of atoms in A and B graphene sublattices.[19,54] Zero-energy states are localized exclusively on the sublattice to which the ZZ edges belong and are exactly degenerate within the nearest-neighbor tight-binding model.[18,19,23] Figure 3 compares the DFT electronic spectra near the Fermi level for the ground states of hydrogen-passivated unreconstructed (ZZ) and reconstructed (ZZ_{57}) TGQDs with $n = 12$. Introduction of the ZZ_{57} edge reconstruction smears the distinction between sublattices. Nevertheless, the zero-energy band survives in a reconstructed (ZZ_{57}) TGQD. As can be seen from the electronic density of occupied states of the band, they are still predominantly localized on the edges. Moreover, the number of zero-energy states remains the same. However, the dispersion of this band increases almost threefold due to reduction of the structure symmetry. Lifting of the band degeneracy becomes observed even in the nearest-neighbor tight-binding model with equal hoppings (not shown), and is more pronounced for the structures in Figs. 1(c) and 1(d), which additionally lift the reflection symmetry present in Fig. 1(b).

Magnetization of the ZZ configuration was investigated in detail through mean-field[18,19] and exact diagonalization[21] calculations. It was shown that the electrons in the zero-energy band are spin polarized. The up- and down-spin edge states are split around the Fermi level such that only up-spin states are filled. Our calculated dispersion of the up-spin states is ~0.03 eV/state [Fig. 3(a)]. On the other hand, the ground state of the ZZ_{57} configuration is antiferromagnetic, i.e., there is no splitting between the up- and down-spin states [Fig. 3(b)]. Nevertheless, calculations for the ferromagnetic ZZ_{57} can still be performed by adjusting the Fermi level for up and down spins independently. The energy spectrum obtained in such a way is similar to the one for ZZ, but with negative Δ_{min}. The interplay of the Δ_{max} and the spin-up band dispersion in such FM calculations can be monitored to predict whether the ground state will be ferromagnetic ($\Delta_{min} > 0$) or antiferromagnetic ($\Delta_{min} < 0$). Apart from the significant increase of the band dispersion, we note that the spin-up and -down splitting Δ_{max} reduces by a factor of 2 in the ZZ_{57} structure. One can see from the charge-density plot in Fig. 3(b) that zero-energy states can now populate both A and B sublattices even close to the center of the dot (see outlined regions). We speculate that the resulting reduction in the peak charge density on each site is responsible for the reduced on-site repulsion between spin-up and spin-down electrons. Stronger dispersion and reduced up-down spin splitting favor kinetic energy minimization versus exchange energy and destroy the ferromagnetism in ZZ_{57}. It should be noted that partial polarization can still be possible in ZZ_{57}. Particularly, we observed it for structures with symmetric corners [Fig. 1(b)], which exhibit smaller dispersion.

Our conclusions based on the analysis of the energy spectra are supported by the total energy calculations depicted in Fig. 4. For the ZZ structure, the gap Δ_{min} is always positive and the total energy of the FM configuration is lower than that of AFM (blue squares). For the ZZ_{57} configuration, on the contrary, the ground state clearly remains AFM for all sizes with the exception of the case with $n = 4$. Here the band consists of only three states and their dispersion can not overcome the splitting between spin-up and spin-down states, resulting in FM configuration being more stable. The total energy difference between the FM and AFM configurations for ZZ remains almost constant (in the range 0.3–0.5 eV) for the triangle sizes studied here, and reduces with size if divided by the number of edge atoms. Such a small value, comparable to the numerical accuracy of the method, makes it difficult to make reliable predictions regarding magnetization of larger dots.

To investigate whether the magnetization of the edges would be preserved on a mesoscale, we plot in Fig. 5 the

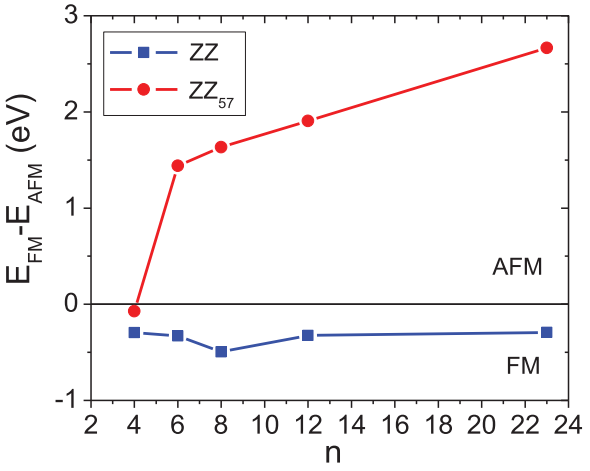

FIG. 4. (Color online) Total energy difference between ferromagnetic and antiferromagnetic states as a function of the size of the triangle for hydrogen-passivated ZZ (blue squares) and ZZ_{57} (red circles). For ZZ, the ground state is ferromagnetic for all sizes studied, while for ZZ_{57}, it is antiferromagnetic for $n > 4$.

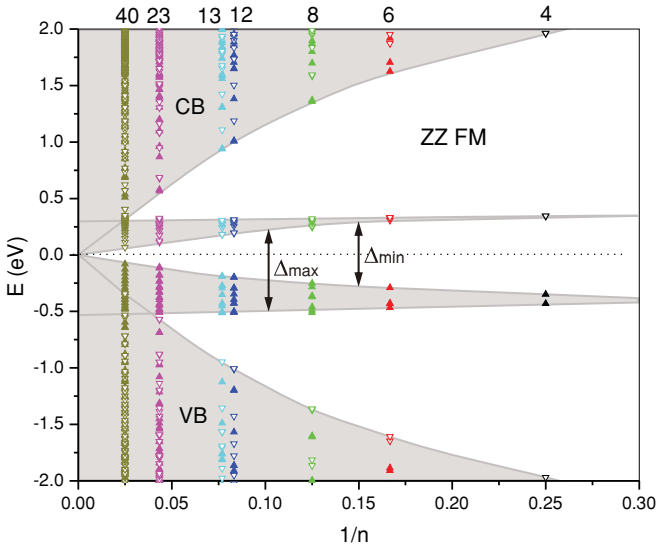

FIG. 5. (Color online) Scaling of the energy gaps with the inverse linear size of ZZ TGQDs. Full energy spectra of the structures calculated in this work are shown. Open symbols correspond to spin-down and filled symbols to spin-up states.

evolution of the energy spectra with the TGQD size. For this plot, we performed an additional calculation for the case of $n = 40$ (1761 carbon atoms total). We did not perform the geometry optimization for this case due to the high computational cost, however, based on the results for smaller structures, we expect that this would have a minor effect on the spectrum. This allows us to notice the reduction of the splitting Δ_{max} between the spin-up and spin-down states with the growing size, which was not appreciated previously.[19] Our GGA gap between zero-energy bands (Δ_{min}) and that between the valence and conduction bands are larger than LDA gaps reported previously,[19] as also observed for graphene nanoribbons.[55] Both gaps show sublinear behavior, complicating the extrapolation to triangles of infinite size. This behavior, however, should change to linear for larger structures where the effect of edges reduces,[22] converging both gaps to zero, as expected for Dirac fermions. An important difference from the nearest-neighbor tight-binding calculation[23] is the growing dispersion of the zero-energy bands. Combined with the reduction of the valence-conduction gap, this leads to the overlap of the zero-energy band with the valence band, even for finite sizes, as indeed observed for the $n = 40$ case (see Fig. 5), while in ZZ_{57} structures, it becomes visible already at $n = 23$ (not shown). Nevertheless, it does not affect the magnetization of the edges, as indeed confirmed by our calculation for $n = 40$, and can be compared to a magnetization of the infinitely long hydrogen-passivated nanoribbons, where the edge state overlaps in energy with the valence band but, in k space, those bands do not actually cross.[8] Our results thus suggest that magnetization of the edges for infinitely large triangles survives in the limit of zero temperature.

In conclusion, we have investigated the relative stability of ZZ and ZZ_{57} edge reconstructions, both with and without hydrogen passivation, in triangular graphene quantum dots. Our results suggest that pentagon-heptagon defects are possible in such dots. The effect of edge reconstruction on electronic and magnetic properties of the dots was investigated as a function of size. The band of zero-energy states is found to survive despite the fact that reconstruction smears out the distinction between the two sublattices. However, the reduction of the dot symmetry due to edge reconstruction is responsible for the increased dispersion (width) of the zero-energy band, while the mixing of sublattices reduces the splitting between spin-up and spin-down bands. These two effects combined destroy the magnetism in dots with reconstructed edges. Nevertheless, for the dots with ideal ZZ edge, spin up-down splitting remains always larger despite the increase of the zero-energy band dispersion with the dot size, and magnetism survives even in the limit of infinitely large dots.

The authors thank M. Korkusinski for fruitful discussions, NRC-CNRS CRP, NRC-NSERC-BDC nanotechnology program, Canadian Institute for Advanced Research, Institute for Microstructural Sciences, and QuantumWorks for support.

[1] K. S. Novoselov, A. K. Geim, S. V. Morozov, D. Jiang, Y. Zhang, S. V. Dubonos, I. V. Grigorieva, and A. A. Firsov, Science **306**, 666 (2004).
[2] K. S. Novoselov, A. K. Geim, S. V. Morozov, D. Jiang, M. I. Katsnelson, I. V. Grigorieva, S. V. Dubonos, and A. A. Firsov, Nature (London) **438**, 197 (2005).
[3] Y. B. Zhang, Y. W. Tan, H. L. Stormer, and P. Kim, Nature (London) **438**, 201 (2005).
[4] S. Y. Zhou, G. H. Gweon, J. Graf, A. V. Fedorov, C. D. Spataru, R. D. Diehl, Y. Kopelevich, D. H. Lee, S. G. Louie, and A. Lanzara, Nat. Phys. **2**, 595 (2006).
[5] A. H. C. Neto, F. Guinea, N. M. R. Peres, K. S. Novoselov, and A. K. Geim, Rev. Mod. Phys. **81**, 109 (2009).
[6] K. Nakada, M. Fujita, G. Dresselhaus, and M. S. Dresselhaus, Phys. Rev. B **54**, 17954 (1996).
[7] K. Wakabayashi, M. Fujita, H. Ajiki, and M. Sigrist, Phys. Rev. B **59**, 8271 (1999).
[8] T. Wassmann, A. P. Seitsonen, A. M. Saitta, M. Lazzeri, and F. Mauri, Phys. Rev. Lett. **101**, 096402 (2008).
[9] L. Yang, M. L. Cohen, and S. G. Louie, Phys. Rev. Lett. **101**, 186401 (2008).
[10] J. Cai *et al.*, Nature (London) **466**, 470 (2010).
[11] B. Wunsch, T. Stauber, and F. Guinea, Phys. Rev. B **77**, 035316 (2008).
[12] J. Wurm, A. Rycerz, I. Adagideli, M. Wimmer, K. Richter, and H. U. Baranger, Phys. Rev. Lett. **102**, 056806 (2009).
[13] A. R. Akhmerov and C. W. J. Beenakker, Phys. Rev. B **77**, 085423 (2008).
[14] F. Libisch, C. Stampfer, and J. Burgdorfer, Phys. Rev. B **79**, 115423 (2009).
[15] Z. Z. Zhang, K. Chang, and F. M. Peeters, Phys. Rev. B **77**, 235411 (2008).
[16] M. Ezawa, Phys. Rev. B **76**, 245415 (2007).
[17] M. Ezawa, Phys. Rev. B **77**, 155411 (2008).

[18] J. Fernandez-Rossier and J. J. Palacios, Phys. Rev. Lett. **99**, 177204 (2007).
[19] W. L. Wang, S. Meng, and E. Kaxiras, Nano Lett. **8**, 241 (2008).
[20] J. Akola, H. P. Heiskanen, and M. Manninen, Phys. Rev. B **77**, 193410 (2008).
[21] A. D. Güçlü, P. Potasz, O. Voznyy, M. Korkusinski, and P. Hawrylak, Phys. Rev. Lett. **103**, 246805 (2009).
[22] A. D. Güçlü, P. Potasz, and P. Hawrylak, Phys. Rev. B **82**, 155445 (2010).
[23] P. Potasz, A. D. Güçlü, and P. Hawrylak, Phys. Rev. B **81**, 033403 (2010).
[24] H. Sahin, R. T. Senger, and S. Ciraci, J. Appl. Phys. **108**, 074301 (2010).
[25] T. Yamamoto, T. Noguchi, and K. Watanabe, Phys. Rev. B **74**, 121409 (2006).
[26] X. Yan, X. Cui, B. Li, and Liang-Shi Li, Nano Lett. **10**, 1869 (2010).
[27] Y. Kobayashi, K. Fukui, T. Enoki, and K. Kusakabe, Phys. Rev. B **73**, 125415 (2006).
[28] O. V. Yazyev and M. I. Katsnelson, Phys. Rev. Lett. **100**, 047209 (2008).
[29] K. A. Ritter and J. W. Lyding, Nat. Mater. **8**, 235 (2009).
[30] E. H. Lieb, Phys. Rev. Lett. **62**, 1201 (1989).
[31] A. Luque and A. Marti, Adv. Mater. **22**, 160 (2010).
[32] A. J. Nozik, Nano Lett. **10**, 2735 (2010).
[33] J. P. Gabor, K. Zhong, M. Bosnick, M. Park, and M. McEuen, Science **325**, 1367 (2009).
[34] R. Baer and E. Rabani, Nano Lett. **10**, 3277 (2010).
[35] J. McClain and J. Schrier, J. Phys. Chem. C **114**, 14332 (2010).
[36] M. D. Watson, A. Fechtenkötter, and K. Müllen, Chem. Rev. (Washington, DC, U.S.) **101**, 1267 (2001).
[37] X. Li, X. Wang, L. Zhang, S. Lee, and H. Dai, Science **319**, 1229 (2008).
[38] C. O. Girit, J. C. Meyer, R. Erni, M. D. Rossell, C. Kisielowski, L. Yang, C. H. Park, M. F. Crommie, M. L. Cohen, S. G. Louie, and A. Zettl, Science **323**, 1705 (2009).
[39] P. Koskinen, S. Malola, and H. Hakkinen, Phys. Rev. B **80**, 073401 (2009).
[40] X. T. Jia, M. Hofmann, V. Meunier, B. G. Sumpter, J. Campos-Delgado, J. M. Romo-Herrera, H. B. Son, Y. P. Hsieh, A. Reina, J. Kong, M. Terrones, and M. S. Dresselhaus, Science **323**, 1701 (2009).
[41] A. Chuvilin, J. C. Meyer, G. Algara-Siller, and U. Kaiser, New J. Phys. **11**, 083019 (2009).
[42] K. Suenaga and M. Koshino, Nature (London) **468**, 1088 (2010).
[43] D. V. Kosynkin, A. L. Higginbotham, A. Sinitskii, J. R. Lomeda, A. Dimiev, B. K. Price, and J. M. Tour, Nature (London) **458**, 872 (2009).
[44] M. Engelund, J. A. Furst, A. P. Jauho, and M. Brandbyge, Phys. Rev. Lett. **104**, 036807 (2010).
[45] B. Krauss, P. Nemes Incze, V. Skakalova, L. P. Biro, K. V. Klitzing, and J. H. Smet, Nano Lett. **10**, 4544 (2010).
[46] L. C. Campos, V. R. Manfrinato, J. D. Sanchez-Yamagishi, J. Kong, and P. Jarillo-Herrero, Nano Lett. **9**, 2600 (2009).
[47] F. Schäffel, J. H. Warner, A. Bachmatiuk, B. Rellinghaus, B. Büchner, L. Schultz, and M. H. Rümmeli, Nano Res. **2**, 695 (2009).
[48] M. Wu, X. Wu, Y. Gao, and X. C. Zeng, J. Phys. Chem. C **114**, 139 (2010).
[49] P. Koskinen, S. Malola, and H. Hakkinen, Phys. Rev. Lett. **101**, 115502 (2008).
[50] C. K. Gan and D. J. Srolovitz, Phys. Rev. B **81**, 125445 (2010).
[51] D. P. Kosimov, A. A. Dzhurakhalov, and F. M. Peeters, Phys. Rev. B **81**, 195414 (2010).
[52] J. M. Soler, E. Artacho, J. D. Gale, A. Garcia, J. Junquera, P. Ordejon, and D. Sanchez-Portal, J. Phys. Condens. Matter **14**, 2745 (2002).
[53] J. P. Perdew, K. Burke, and M. Ernzerhof, Phys. Rev. Lett. **77**, 3865 (1996).
[54] S. Fajtlowicz, P. E. John, and H. Sachs, Croat. Chem. Acta **78**, 195 (2005).
[55] E. Rudberg, P. Salek, and Y. Luo, Nano Lett. **7**, 2211 (2007).